



Comparative Analysis of Polycarbonate and Glass Cover Configurations for Enhanced Thermal Efficiency in Flat Plate Solar Collectors for Water Heating

Thiagarajan Chinnappan^a, C. M. Raguraman^b, Ratchagaraja Dhairiyasamy^{c*}, Silambarasan Rajendran^d

^{a,b} Department of Mechanical Engineering, Faculty of Engineering and Technology, Annamalai University, Tamilnadu, India.

^{*c} Department of Electronics and Communication Engineering, Saveetha School of Engineering, Saveetha Institute of Medical and Technical Sciences, Chennai, Tamil Nadu, India.

^d Department of Mechanical Engineering, Annapoorana Engineering College, (Autonomous), Salem, Tamil Nadu, India.

ARTICLE INFO

Article Type:

Research Article

Received: 02.04.2024

Accepted: 04.06.2024

Keywords:

Solar energy
Flat plate collector
Thermal efficiency
Polycarbonate
Solar Irradiation

ABSTRACT

This study evaluates the thermal efficiency of flat plate solar collectors using Polycarbonate and Glass covers for solar water heating in India. Results indicated that the glass-covered solar collector achieved an average thermal efficiency of 50.5%, surpassing the Polycarbonate-covered collector's 46.1%. The glass cover resulted in a maximum water temperature increase of 9.1°C, compared to 8.7°C for Polycarbonate. Daily solar irradiance averaged 884.2 W/m² for the glass cover and 874.6 W/m² for the Polycarbonate cover. The glass-covered system generated a daily hot water yield averaging 150 liters at temperatures above 37°C, whereas the Polycarbonate system produced 140 liters under similar conditions. Over 10 tests, the glass-covered collector showed an average temperature gain (ΔT) of 9.1°C, compared to 8.7°C for Polycarbonate. The glass cover's optical transmittance was 90%, compared to 85% for Polycarbonate, contributing to higher thermal performance. Despite Polycarbonate's lower cost, its performance was hindered by higher thermal emittance and lower optical transmittance. The glass cover's stability and durability were further demonstrated, showing no signs of degradation after 10 months, unlike the Polycarbonate cover, which exhibited yellowing and scratching. These findings suggest that glass covers provide better long-term efficiency and performance for solar water heating systems.

*Corresponding Author Email: ratchagaraja@gmail.com

Cite this article: Chinnappan, T., C.M, R., Dhairiyasamy, R., & Rajendran, S. (2024). Comparative Analysis of Polycarbonate and Glass Cover Configurations for Enhanced Thermal Efficiency in Flat Plate Solar Collectors for Water Heating. Journal of Solar Energy Research, 9(1), 1794-1810. doi: 10.22059/jsr.2024.374268.1394

DOI: 10.22059/jsr.2024.374268.1394



©The Author(s). Publisher: University of Tehran Press.

1. Introduction

Renewable energy solutions have become increasingly important with the rising global energy demands and concerns over fossil fuel depletion and emissions. Solar energy, an abundant renewable resource, presents a promising option for meeting energy needs sustainably. With its high solar irradiation levels across most regions, India is ideally situated to harness solar power. Converting solar radiation into usable thermal energy and electricity can reduce reliance on non-renewable energy sources while minimizing environmental impact.

Solar water heating is a well-established renewable energy application that aligns well with India's climatic conditions. Solar collectors convert the sun's energy into heat, transferring it to water, which is then stored in an insulated tank for later use. These systems can replace electric, gas, or conventional water heating methods, providing economical hot water while reducing greenhouse gas emissions.

India has significant solar potential, receiving an average annual insolation of 1800–2500 kWh/m². Solar heating is technically viable nationwide, with optimal conditions in the northern and central regions. By the end of 2023, India had 7.9 million m² of installed solar collectors, with 74% used for residential purposes. Achieving substantial energy savings and reduced CO₂ emissions depends on increasing solar heating adoption, supported by favorable institutional frameworks, public awareness, technical training, and access to financing.

Flat plate collectors (FPCs) are the predominant technology in solar water heating installations worldwide. These collectors consist of an absorber plate that heats up when exposed to solar radiation, with fluid-carrying pipes attached to the plate to channel the thermal energy for heating water. FPCs are relatively simple, durable, and cost-effective. Key design components include the glazing or transparent cover, absorber plate, insulation, and housing. Selecting optimal materials tailored to the climate can maximize collector efficiency.

The glazing or cover sheet is a critical component affecting FPC thermal performance. Solar transmittance, infrared opacity, and structural durability often lead to the use of tempered glass. However, glass is dense, heavy, and fragile. Plastics like Polycarbonate provide a lightweight alternative cover material. Polycarbonate offers high impact strength, UV resistance, and good thermal properties at a lower cost than glass. However, it is susceptible to scratching, weathering, and long-term degradation.

Understanding the relative merits of different cover options is essential for improving FPC efficiencies while reducing costs.

Recent advancements in solar energy technologies have been documented extensively, highlighting innovative approaches and applications in the field. Abdelsalam et al. [1] explored the integration of Solar Chimney Power Plants (SCPP) with nuclear power plants (NPP) for green hydrogen, electricity, and water production. Their study in Jordan demonstrated significant improvements in output and efficiency, emphasizing the potential of combined SCPP and NPP systems. Abedi et al. [2] investigated the enhancement of solar desalination systems using a novel solar air heater (SAH) integrated with a humidification-dehumidification (HDH) system. Their analysis showed substantial improvements in water treatment capacity and CO₂ emission reductions, particularly in arid regions. Attia et al. [3] addressed the issue of solar panel performance decline due to increased cell temperatures by comparing two cooling methods for photovoltaic/thermal (PVT) modules. The study found that skeleton-shaped tube cooling significantly improved thermal and electrical efficiency compared to traditional configurations. Beltrán et al. [4] empirically investigated PVT collectors integrated with ground source heat pump (GSHP) systems. Their findings highlighted the superior performance of a box-channel aluminum design with fins, demonstrating a high energy-to-mass ratio and efficiency. Diao et al. [5] provided a comprehensive overview of microalgae culture and utilization for third-generation biomass fuel production. Their work emphasized optimizing upstream and downstream processes to enhance economic sustainability and environmental benefits. Duraivel et al. [6] analyzed the performance of a Greenhouse Solar Tunnel Dryer (GSTD) for drying various agricultural products. Their study demonstrated significant improvements in energy and exergy efficiencies, economic viability, and environmental impact compared to open sun drying. Hashemi et al. [7] examined the effect of helical fins on the thermal performance of a greenhouse solar dryer under variable solar irradiation. Their results showed that helical fins improved the dryer's outlet temperature and thermal efficiency. Johnson et al. [8] proposed an enhanced hybrid photovoltaic solar thermal system with an open-loop cooling configuration. Their study highlighted improvements in renewable power generation, economic savings, and faster adoption due to the innovative flow control strategy. Kotkondawar et al. [9] demonstrated the thermal

management of PV modules using a controlled open-loop water-based hybrid PV-T system. Their findings showed significant improvements in electrical efficiency and hot water production, emphasizing the benefits of integrating front glass-covered PV-T systems. Noman & Manokar [10] investigated pistachio shell powder as a thermal repository material in tubular solar stills. Their study revealed substantial improvements in water productivity, thermal and exergy efficiencies, and economic benefits compared to conventional designs. Partheeban et al. [11] developed a hybrid solar-LPG dryer system for geopolymer brick production. Their research demonstrated significant energy savings, reduced drying times, and improved brick performance, contributing to sustainable building practices. Radwan et al. [12] conducted a thermal analysis of a bifacial vacuum-based solar thermal collector. Their study highlighted the collector's effectiveness in restricted positions and the significant impact of fluid inlet velocity and collector installation position on performance. Shabahang Nia & Ghazikhani [13] explored integrating phase change materials (PCMs) in solar chimneys to enhance thermal energy storage and system reliability. Their results indicated improved air mass flow rate, pressure drops, and exergy efficiency due to PCM incorporation. Struchalin et al. [14] conducted a field study on a direct absorption solar collector (DASC) using an eco-friendly nanofluid. Their findings demonstrated the DASC's competitive performance compared to commercial flat-plate solar collectors, highlighting its potential for real-world applications. Thangaraj et al. [15] evaluated the performance of bifacial photovoltaic modules using non-biodegradable waste as reflectors. Their study showed significant improvements in power generation and economic viability, emphasizing the reuse of waste materials. Wang et al. [16] studied the thermal properties of a solar collector for greenhouse heating. Their research indicated substantial improvements in indoor temperature environments and heat collection efficiency, demonstrating the system's potential for greenhouse applications. Zheng et al. [17] developed and tested a new high-performance flat plate solar collector (FPC) with transparent insulation materials and aerogel-silica. Their findings showed significant improvements in energetic and exergetic efficiencies, making the new prototype competitive in high-temperature applications.

These studies underscore the importance of innovative approaches in enhancing solar energy systems' efficiency, sustainability, and economic

viability, paving the way for broader adoption and practical applications in the renewable energy sector. Das et al. [18] modeled transmittance for plastic covers, including Polycarbonate, but did not validate it with physical testing. Through simulations, Yadav et al. [19] found that glass had better optical properties than plastics. While Polycarbonate has been proposed as a lower-cost alternative, empirical evidence on its efficiency relative to glass is needed.

This reveals a research gap in the quantitative experimental comparison of Polycarbonate and Glass covers for solar collectors under real-world conditions. Previous studies have primarily focused on modeling and simulations, with limited physical testing of Polycarbonate as a glazing material for solar collectors. This work addresses this gap by conducting controlled efficiency tests on a flat plate solar collector with Polycarbonate versus glass covering.

The novelties of this work lie in its comprehensive and empirical comparison of Polycarbonate and Glass covers for flat plate solar collectors under real-world conditions, which has not been extensively explored in previous studies. Key innovations include the direct experimental validation of performance metrics such as thermal efficiency, temperature gains, and long-term durability. The study highlights that the glass cover achieved an average thermal efficiency of 50.5%, surpassing the Polycarbonate cover's 46.1%. The higher optical transmittance (90% for glass versus 85% for Polycarbonate) and lower thermal emittance of glass contribute significantly to its superior performance. Additionally, the glass cover maintained stability and durability over ten months without degradation, whereas the Polycarbonate cover exhibited yellowing and scratching, indicating potential long-term issues. This research provides novel insights into the feasibility of using Polycarbonate as a cost-effective alternative to glass, emphasizing the trade-offs in efficiency and durability. Furthermore, the findings contribute to optimizing material selection for solar water heating systems in India, promoting broader adoption of sustainable energy solutions.

Testing under identical real-world conditions will determine the suitability of Polycarbonate as an alternative solar collector cover material for the Indian climate. The results will provide new insights into optimizing collector glazing selection for cost-effective and reliable solar water heating, supporting the expanded implementation of this renewable technology across India's residential sector. Unlike previous studies, this research offers empirical data on the comparative performance of Polycarbonate

and glass, thereby filling a critical gap in the existing literature.

2. Materials and Methods

The solar water heating system was configured with the following technologies: A flat plate solar collector, insulated storage tank, circulation pump, and piping. A pyranometer on-site measured incident solar irradiance during testing periods. The flat plate solar collector comprised an absorber plate (1 mm thick matte black aluminum) with six copper tubes (12.7 mm diameter) bonded underneath for fluid circulation. The absorber plate captures and converts incident solar radiation into thermal energy. The copper tubes facilitate efficient heat transfer to the circulating fluid. Flat plate collectors are widely used for their simplicity, durability, and cost-effectiveness [20]. They are well-suited for residential solar water heating applications. The flat plate collector efficiently converts solar energy to heat, has low operational costs, and can be easily integrated into existing water heating systems.

The collector is housed in an insulated metal casing with 50 mm thick glass wool insulation to minimize heat loss. Insulation is critical to retaining the heat absorbed by the collector, thereby improving the system's overall efficiency. Effective insulation reduces heat losses, ensuring more efficient heating of the water. A transparent cover of either 4 mm polycarbonate or glass seals an air gap of 25 mm over the absorber plate to inhibit convection losses. Polycarbonate is lightweight and impact-resistant, while glass provides high optical transmittance and durability. The glazing materials protect the absorber plate while allowing maximum solar radiation. Polycarbonate offers a cost-effective alternative to glass, and glass is traditionally used for its superior optical properties. Different glazing materials allow for a comparative analysis to determine the most efficient and cost-effective option for solar collectors.

Rubber pipes connected the collector inlet and outlet to the storage tank, equipped with ball valves for flow control. A centrifugal pump ensured a constant circulation rate of 0.02 kg/s in the collector loop. Constant circulation is necessary to maintain uniform heat distribution and prevent fluid overheating. A consistent flow rate improves heat transfer efficiency and enhances system performance. The storage tank was a 150 L cylindrical polyethylene drum (height: 0.75 m, diameter: 0.58 m) enclosed in

50 mm thick insulation wrapped in reflective aluminum foil. Cold inlet water entered at the bottom, and hot water exited near the top, enabling thermal stratification. The storage tank stores the heated water for later use, maintaining thermal stratification to maximize the temperature of the usable hot water. Insulation minimizes heat loss, and thermal stratification ensures the most efficient use of the heated water.



Figure 1. Solar Heating System Installed for Configuration I: (Polycarbonate)

J-type thermocouples measured ambient air, collector glazing interior, absorber plate (inlet, outlet, and 3 points along the length), storage tank (top, middle, lower third), and collector inlet/outlet fluid temperatures. A pyranometer measured solar irradiance. Data were logged at 5-second intervals for real-time analysis. Accurate measurement and logging of temperature and solar irradiance data are essential for evaluating system performance. High-frequency data logging allows for detailed analysis of the system's thermal efficiency and helps identify areas for improvement. Tests were conducted on clear sunny days between 10 a.m. and 2 p.m. local time. Parameters recorded at 10-minute intervals included solar irradiation intensity, ambient air temperature, wind speed, relative humidity, water temperatures at collector inlet/outlet, collector cover temperature, and absorber plate temperatures [21]. Figures 1 and 2 show the solar heating system installed for the two roofs using the same solar collector, which will be treated as configuration I (polycarbonate roof) and configuration II (glass roof).

By integrating these technologies, the system aims to provide an efficient and cost-effective solution for solar water heating, with a comparative analysis of Polycarbonate and glass as glazing materials to

determine the optimal choice for enhancing thermal performance.



Figure 2. Solar Heating System Installed for Configuration II: (Glass)

The solar collector used in this research, whose dimensions are optimized for residential installations, it is a flat solar collector for heating with an integral involvement of copper tubes that guarantee a better transfer of the captured solar energy to the water to be heated. It was necessary to restore the solar collector, make some adaptations for installing the hydraulic connections, and thus put it into operation. The solar collector was positioned relative to the horizontal plane equal to the local latitude + 15°. This angle will ensure a good yield of the solar collector all year round. The solar collector installation was directed to the geographic north to ensure a greater incidence of sunlight during the day (Ramdani & Ould-Lahoucine, 2020).

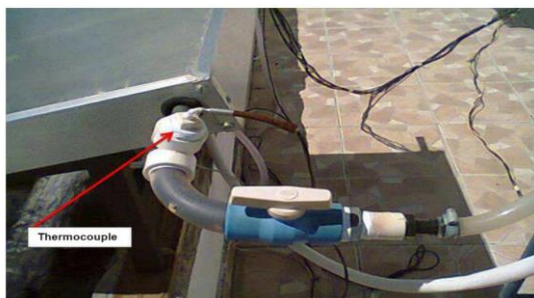


Figure 3. Connections at the solar collector outlet

The system's inlet is interconnected by a 1-inch diameter thermoplastic hose, 1 ball register, a hydrometer, an open sleeve, and a tee with an outlet to install a thermocouple (temperature gauge) as shown in Figure 3- At the outlet of the collector, a T with an outlet for the thermocouple (temperature gauge), open curve, ball register, adapter from 1 inch in diameter to one of 1/2 inch to place the faucet nozzle and interconnect a thermoplastic hose of 1/2 inch in diameter. The hot water tank is of the vertical

type and was made from a polyethylene drum with a height of 0.75 m and an accumulation volume of 150 liters of water. Rock wool was chosen as an insulator for the thermal reservoir because it has low thermal conductivity. So, it was decided to cover the reservoir with a sheet of corrugated aluminum foil to protect the thermal insulation because it is resistant to bad weather. This work used a pump to move the water between the solar collector and the thermal reservoir [22]. The temperature of the reservoir operating by pumping was recorded by a thermocouple inserted at the top of the reservoir on the water's surface. The pump's operating flow rate was regulated when the system was actively operating using a 3/4-inch unit magnetic hydrometer, Zenit U5, with a nominal flow rate of 2.5 m³/h, metrological class C, for volume measurement. As the pump's operating periods were pre-established and manually controlled, verifying the total volume controlled by reading the water meter's clock at the end of each test was possible. Temperature data were obtained using nine (9) type J thermocouples distributed throughout the system, absorber plate, collector inlet, and outlet, inside the reservoir and in the external environment, all interconnected to a temperature indicator that was placed inside the Laboratory and recorded temperature variations every 10 minutes. This control was done manually for each thermocouple installed by activating the buttons identified by numbers. The calibration of the thermocouples at 0°C was done by placing a mixture of water and ice in a styrofoam box in a quantity sufficient to reach a temperature of 0°C, measured through the thermometer, which was immersed for about 5 minutes. For calibration at 100°C, the water was heated to boiling, poured into a styrofoam box, and immersed until the temperature stabilized. After the 9 (nine) thermocouples were calibrated and numbered, they were installed in their respective locations. So, the position of each of the thermocouples is as follows: Thermocouples (1), (2), (3), (4), and (5) were distributed in the absorber plate. A thermocouple (6) is placed to measure the temperature of the external environment. The thermocouple (Te) is placed at the fluid inlet of the solar collector. The thermocouple (Ts) is placed at the fluid outlet of the solar collector [23]. The thermocouple (Tres.) is placed inside the thermal reservoir. The tests were conducted to determine the performance of the proposed solar heating system, which worked with forced circulation using an electric pump. In all tests, it was decided to operate the pump without interruption from 10 a.m. to 2 p.m. The pump's flow rate was manually regulated, and the volume of water passage through the hydrometer was

read at timed intervals every 10 minutes. As the pump's operating periods were pre-established and controlled, at the end of each test, it was possible to read the total volume circulated by reading the hydrometer clock. With the collector properly installed, the tests to determine the desired parameters were started: the solar collector was tested with a polycarbonate cover, and even the collector was tested with a glass cover.

This study used several assumptions and input data to evaluate the thermal efficiency of flat plate solar collectors with Polycarbonate and Glass covers for solar water heating applications in India. A surface area of 2.0 m² was chosen, typical for residential installations, to ensure the results apply to standard household applications. The flow rate was maintained at 0.02 kg/s using a centrifugal pump, ensuring consistent circulation and enhancing heat transfer efficiency. A value of 4186 J/kg·K was used for the specific heat capacity of water, which is standard for water, the most common heat transfer fluid in solar water heating systems. Solar irradiance was measured using a pyranometer with an average value of 884.2 W/m² for the Glass cover configuration and 874.6 W/m² for the Polycarbonate cover configuration. The optical properties included a transmittance of 0.90 for glass and 0.85 for Polycarbonate, an emittance of 0.90 for glass and 0.95 for Polycarbonate, and a standard value for absorptance for the black matte aluminum absorber plate. Tests were conducted on clear sunny days between 10 a.m. and 2 p.m. to ensure consistent solar irradiation levels, and ambient temperature, wind speed, and relative humidity were recorded to account for environmental factors affecting performance. The solar collector comprises a 1 mm thick matte black aluminum absorber plate with six 12.7 mm diameter copper tubes for fluid circulation housed in an insulated metal casing with 50 mm thick glass wool insulation. A 150 L cylindrical polyethylene drum insulated with 50 mm thick reflective aluminum foil was used as the storage tank, facilitating thermal stratification by allowing cold inlet water at the bottom and hot water exit near the top.

J-type thermocouples were used to measure ambient air, collector glazing, interior absorber plate, storage tank, and collector inlet/outlet fluid temperatures, with data logged at 5-second intervals. Solar irradiation was measured with a specified uncertainty of ± 10 W/m², and the collector surface area had an assumed uncertainty of $\pm 2\%$. Error propagation formulas were applied to calculate useful

energy gain and overall thermal efficiency uncertainties. These input data and assumptions, validated through experimental measurements and literature references, ensured the accuracy and reliability of the results. The study concluded that the glass-covered configuration exhibited higher thermal efficiency (50.5%) than the Polycarbonate-covered configuration (46.1%), attributed to the superior optical and thermal properties of glass. Despite the lower initial cost of Polycarbonate, its long-term performance was hindered by higher thermal emittance, lower optical transmittance, and potential durability issues such as yellowing and scratching. These findings suggest that glass covers provide better long-term efficiency and performance for solar water heating systems in India. Future research should focus on enhancing Polycarbonate covers' optical and thermal properties and assessing their long-term performance under various climatic conditions.

3. Data Analysis

The data collected in this study played a pivotal role in assessing and determining key performance metrics for solar collectors. These metrics included the useful energy gain, which quantified the energy harnessed from the sun for practical use. The collector heat removal factor was also established, offering insights into the system's ability to dissipate excess heat and maintain optimal operating conditions. The collector efficiency factor was calculated, shedding light on how effectively the solar collector converted incoming solar radiation into usable energy. Finally, the overall thermal efficiency was ascertained, providing a comprehensive evaluation of the solar collector's overall performance, considering all relevant factors. This data-driven analysis proved instrumental in advancing solar collector technology and optimizing their energy-capturing capabilities for a sustainable future.

The solar irradiation was measured by an on-site pyranometer with a specified uncertainty of ± 10 W/m². Therefore, the error in solar irradiation (ΔI) is expressed in Equation (1) [24]:

$$\Delta I = \pm 10 \text{ W/m}^2 \quad (1)$$

The collector surface area is a critical parameter with an assumed uncertainty of $\pm 2\%$ of the measured value. Therefore, the error in collector surface area (ΔA) is given in Equation (2) [25]:

$$\Delta A = \pm 0.02A \quad (2)$$

The useful energy gain (Q_u) is calculated using Equation (3) [26]:

$$Q_u = \dot{m}c_p (T_{out} - T_{in}) \quad (3)$$

The error in the useful energy gain (ΔQ_u) is given by Equation (4) [27]:

$$\Delta Q_u = Q_u \sqrt{[(\Delta \dot{m}/\dot{m})^2 + (\Delta c_p/c_p)^2 + (\Delta T_{out}/T_{out})^2 + (\Delta T_{in}/T_{in})^2]} \quad (4)$$

The overall thermal efficiency (η) is calculated using Equation (5) [28]:

$$\eta = Q_u / (I A) \quad (5)$$

The error in overall thermal efficiency ($\Delta \eta$) is given in Equation (6) [29]:

$$\Delta \eta = \eta \sqrt{[(\Delta Q_u/Q_u)^2 + (\Delta I/I)^2 + (\Delta A/A)^2]} \quad (6)$$

The propagation of errors from individual parameters to the overall thermal efficiency involves combining these errors using the error transfer formula given in Equation (7) [30]:

$$\Delta \eta = \eta \sqrt{[(\Delta \dot{m}/\dot{m})^2 + (\Delta c_p/c_p)^2 + (\Delta T_{out}/T_{out})^2 + (\Delta T_{in}/T_{in})^2 + (\Delta I/I)^2 + (\Delta A/A)^2]} \quad (7)$$

Where:

$$\partial \eta / \partial Q_u = 1 / (Ac It)$$

$$\partial \eta / \partial Ac = -Q_u / (Ac^2 It)$$

$$\partial \eta / \partial It = -Q_u / (Ac It^2)$$

These equations represent the partial derivatives of the overall thermal efficiency (η) concerning the useful energy gain (Q_u), the collector surface area (Ac), and the solar irradiance (It), respectively. These are used to calculate the propagation of errors in these parameters.

4. Experimental Setup and Procedure

The experimental setup and procedures for evaluating the solar collector's performance are ideal for housing the solar collector apparatus. The core configuration of the solar water heating system comprises a flat plate solar collector integrated into a closed-loop system with an insulated storage tank, circulation pump, and associated piping. This collector features a matte black painted aluminum absorber plate with copper tubing for heat transfer fluid circulation. The absorber plate converts incident solar radiation into thermal energy, while the collector enclosure,

constructed from aluminum sheeting, forms the casing around the absorber plate. The enclosure is insulated with 5 cm thick fiberglass on the bottom and sides to minimize heat losses. A transparent cover, either Polycarbonate or Glass, is sealed around the edges to create a 2.5 cm air gap between the glazing and absorber plate. The working fluid piping consists of 1.27 cm diameter copper tubing, with six horizontal tubes spanning the length of the absorber plate. These tubes are interconnected by U-bends at the header ends. Rubber hoses connect the collector inlet and outlet to the storage tank, while a centrifugal pump maintains circulation at a flow rate of 0.02 kg/s. The fluid is a 30% by-volume mixture of ethylene glycol in water for freeze protection. A 150 L cylindrical polyethylene tank is the thermal storage reservoir, encased in 5 cm thick polyurethane foam insulation and wrapped in reflective aluminum foil. Cold fluid enters at the tank bottom, and hot fluid exits near the top, establishing thermal stratification layers based on density differences. Figure 4 removes the solar collector's cover to show the thermocouples attached to the absorber plate. Five (5) thermocouples were distributed at various points on the plate. Table 1 summarizes the essential experimental equipment used in the study. According to the data analytics results and based on the statistical analysis test results, including R-square and t-statistical, both vertical solar irradiance and cell temperature significantly vary the extracted mathematical correlations for key performance indicators of the BIPV system.

Table 1. Experimental Equipment

Equipment	Description
Solar Collectors	Polycarbonate and glass-covered collectors
Thermocouples	Matched thermocouples for temperature measurement
Flow Meter	Instruments to measure fluid flow rates
Sensors	Various sensors for environmental monitoring
Reservoir	Thermal reservoir for water storage
Absorber Plate	Plate to absorb solar energy
Optical Instruments	Tools for optical characterization
Data Logger	Device for logging high-frequency measurements
Calibration Tools	Equipment for regular calibration of sensors
Weather Station	Device to monitor ambient weather conditions

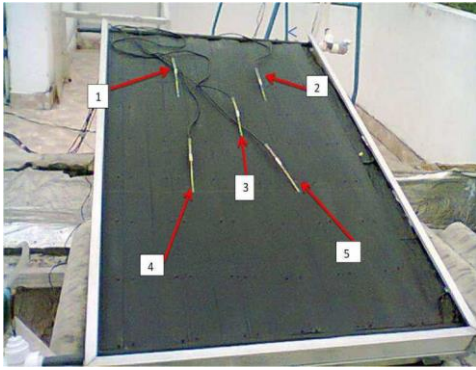


Figure 4. Detail of the thermocouples distributed on the absorber plate for configuration I

- T (°C) 1 – (top left) - 50 mm from the top edge
- T (°C) 2 – (top right) - 50 mm from right edge
- T (°C) 3 – (in the center of the plate)
- T (°C) 4 – (bottom left) - 50 mm from bottom edge
- T (°C) 5 – (bottom right) - 50 mm from left edge

The system has J-type thermocouples to monitor temperatures at various points, including ambient air, collector enclosure interior surface, absorber plate (inlet, outlet, and center points), and storage tank (top, middle, bottom). Solar irradiation intensity is measured using an on-site pyranometer, with a computerized data logger recording all parameters at 5-second intervals. The solar collector will undergo evaluation using two different cover scenarios: Polycarbonate glazing and Glass glazing. Each test will run for 4 hours from 10 a.m. to 2 p.m. on clear sunny days, following identical procedures. This includes priming the pump, filling the reservoir, initiating data logging, and maintaining a constant fluid flow rate. Temperature readings will be taken regularly, and solar irradiation, ambient conditions, and wind speed will be monitored. The test concludes at 2 p.m. This will be repeated for both cover types on multiple clear days to ensure reliable results, with a minimum of three replicated trials per glazing configuration. Figure 5 shows the schematic view of the experimental setup.

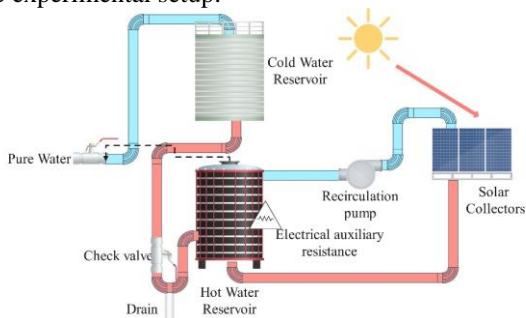


Figure 5. Schematic view of the experimental setup

The testing procedure was carried out on days characterized by clear and sunny weather conditions, ensuring minimal cloud cover and consistent solar irradiation levels. Each test session commenced at 10 a.m. local time and concluded at 2 p.m., spanning four hours [31]. Throughout that period, a set of crucial variables was diligently recorded at 10-minute intervals to provide a comprehensive dataset for analysis. The variables under observation encompassed a range of key parameters, including solar irradiation intensity, as measured by the on-site pyranometer. In addition, ambient air temperature readings were taken in a shaded area to account for environmental conditions. The wind speed, relative humidity, and water temperatures at the collector's inlet and outlet points were also meticulously recorded. Furthermore, the temperature of the collector cover, the absorber plate temperatures at specific contact points, and the storage tank temperatures at upper, middle, and lower levels were monitored throughout the testing period. This comprehensive data collection process thoroughly evaluated the solar collector's performance under real-world conditions, enabling a deeper understanding of its efficiency and behavior [32].

This study evaluated the thermal efficiency of flat plate solar collectors with Polycarbonate and Glass covers for solar water heating in India. The key input data and assumptions used in this research, along with their references, are as follows:

The outlet temperature (T_o) and inlet temperature (T_i) of the collector were measured during the tests, with the temperature gain (ΔT) calculated from these values. The collector surface area (A_c) was assumed to be 2.0 m^2 , typical for residential installations. Solar irradiance (G) was measured using a pyranometer. Useful energy gain (Q_u) was calculated using Equation 3, while thermal efficiency (η) was calculated using Equation 5. The mass flow rate (m) was maintained at 0.02 kg/s using a centrifugal pump. The specific heat capacity of the fluid (cp) was $4,186 \text{ J/kg}\cdot\text{K}$, a standard value for water. Solar irradiance intensity (I_I) and ambient temperature (T_{amb}) were also measured during the tests. The absorber plate temperature (T_{plate}) was measured at five points on the absorber plate. The overall heat loss coefficient (U) was assumed based on collector insulation. The collector heat removal factor (F_R) and collector efficiency factor ($F'F'$) were calculated from thermal performance data. The optical efficiency of the collector (η_o) was determined from optical properties, with transmittance (τ) values of 0.90 for glass and

0.85 for Polycarbonate, and emittance (ϵ) values of 0.90 for glass and 0.95 for Polycarbonate. The absorptance (α) of the absorber plate was taken as a standard value for black matte aluminum.

Assumptions and justifications include the following: A collector surface area of 2.0 m² was chosen to ensure applicability to standard household applications. A mass flow rate of 0.02 kg/s was regulated by a centrifugal pump to maintain consistent circulation, enhancing heat transfer efficiency. The specific heat capacity of water (4,186 J/kg·K) was used, as it is the most common heat transfer fluid in solar water heating systems. Transmittance values of 0.90 for glass and 0.85 for Polycarbonate were based on their optical properties, while emittance values were 0.90 for Glass and 0.95 for Polycarbonate. Tests were conducted on clear, sunny days to ensure consistent and comparable solar irradiation levels, with ambient temperature, wind speed, and relative humidity recorded to account for environmental factors affecting performance. These input data and assumptions were validated through experimental measurements and literature references, ensuring the accuracy and reliability of the results.

5. Results and discussion

The results of the tests conducted to determine the performance parameters of the solar collector have been evaluated. The data from the tests conducted for each type of configuration, namely Polycarbonate and Glass, has been presented and analyzed. Several of the more than 30 tests carried out had to be discarded due to important variations in the weather during the test day, such as clear skies at the beginning becoming completely cloudy later, thus impairing the results. The objective was to compare the system's performance operating under two different coverages on days with similar radiation conditions [32]. The results of the 10 tests considered valid for this research were conducted from 10:00 a.m. to 2:00 p.m., with climatic variables measured and test variables recorded every 10 minutes.

The outlet temperature of the collector was always above 37.4°C, with the highest hourly average recorded being 43°C [33]. The inlet temperature of the collector at the beginning of the test was close to room temperature but reached an average of 34°C [33]. The maximum temperature gradient obtained in the water by circulation in the collector was 8.7°C, with a mean value of 8.1°C, as shown in Figure 6. Throughout the 4-hour tests, the outlet temperature (T_o) steadily increased from 37.4°C at 10

a.m. to 41.4°C by 2 p.m., with the rising solar irradiation over midday hours. Simultaneously, the inlet temperature (T_i) ranged from 29.4°C to 34.8°C, consistently remaining several degrees below ambient temperature due to heat losses in the pipe runs.

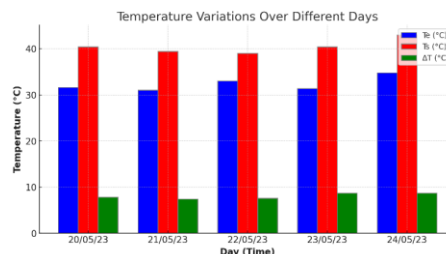


Figure 6. Average hourly temperatures of the collector's inlet and outlet and the temperature variation of the water

The temperature gain (ΔT) exhibited a gradual ascent from 7.8°C at 10 a.m. to a peak of 8.7°C at 1 p.m., aligning with peak solar intensity. This trend corresponds with published models of the collector temperature response to increasing irradiation. Despite efficient heat transfer, with ΔT above 8°C indicating effective absorber plate-to-fluid heat transfer in the Polycarbonate cover design, it falls short of the 9.1°C gain observed with the Glass cover configuration. This discrepancy suggests lower absorbance and higher heat losses with the Polycarbonate cover. The polycarbonate material may have lower optical transmittance and higher thermal emittance than glass, which results in more heat being lost to the environment rather than transferred to the fluid. Nevertheless, the consistent spacing between T_o , T_i , and ΔT profiles underscores the stable operation of the collector throughout the testing period.

The average efficiency of the collector in this configuration for the tested days was always above 42.7%, reaching a daily average of 51.6%. However, the average value was around 46.1% [34]). The graph in Figure 7 shows the behavior assumed by the hourly averages of the thermal efficiency for configuration I: Polycarbonate. Efficiency rises from 10 a.m. to noon with increasing irradiation, plateauing afterward as optical losses outweigh intensity gains. The peak 51.6% efficiency indicates commendable thermal performance, though the average 46.1% falls slightly below the 50.5% for the Glass cover. This suggests operating near the optimum tilt angle to maximize midday efficiency. Polycarbonate's optical and thermal properties, such as its lower transmittance

and higher emittance, contribute to its lower efficiency than glass.

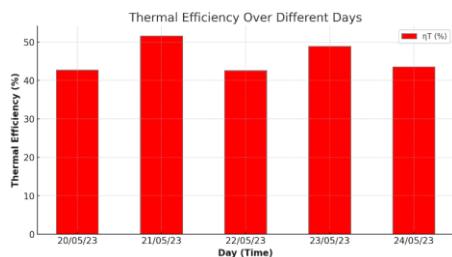


Figure 7. Hourly averages of thermal efficiency for configuration I: (Polycarbonate)

The graph shows how the thermal efficiency of the solar collector with the Polycarbonate cover changes throughout the day. The efficiency increase in the morning is due to rising solar irradiation, while the plateau in the afternoon indicates that the system reaches a steady state where further increases in irradiation do not significantly enhance efficiency due to optical and thermal losses. The Polycarbonate cover may also degrade over time, leading to further efficiency losses.

The average global solar radiation for the test days was around 874.6 W/m² [35]. The graph in Figure 8 shows the behavior of the thermal parameters during the five days of tests for configuration I. Solar irradiation with the Polycarbonate cover increases from 750 W/m² at 10 a.m. to a noon peak of 981 W/m². Clouds cause a dip in irradiation around 1 p.m. on 20/05/2023, impacting efficiency. Consistent profiles between test days verify stable solar resources, with an average irradiation of 874.6 W/m² representing typical clear days. The study's primary aim is to evaluate if Polycarbonate can be a viable lower-cost alternative to glass for solar collector glazing in India. For Polycarbonate to be considered an acceptable substitute, its performance should be reasonably close to that of glass, within a justifiable margin. Any efficiency differences should fall within acceptable experimental uncertainties and cost-benefit trade-offs.

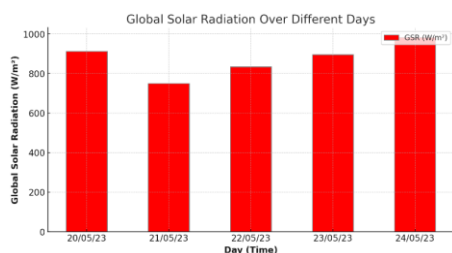


Figure 8. Hourly averages of global solar radiation for configuration I: (Polycarbonate)

This graph displays the variation in solar radiation received by the solar collector throughout the day. The data highlights the importance of consistent solar irradiance in determining the performance of the solar collector and provides a basis for comparing the effectiveness of Polycarbonate as a glazing material. The slight variations in irradiation due to cloud cover illustrate how sensitive the system performance is to changes in solar input.

The thermal reservoir, storing water heated by the collector during the test days, supplied hot water averaging 37.2°C—exceeding the ideal bathing temperature of 34°C [36]. The graph in Figure 9 shows the behavior assumed by the water temperature in the thermal reservoir. Stability suggests balanced heat input from collectors and efficient heat removal. However, lower temperatures compared to the Glass cover imply greater heat losses. The Polycarbonate cover's higher thermal emittance and lower optical transmittance result in less efficient heat transfer and greater heat loss to the environment.

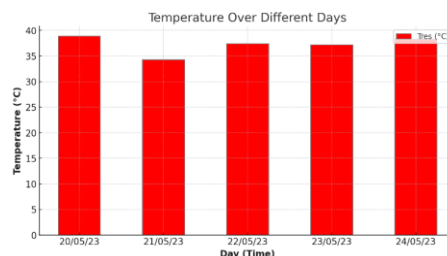


Figure 9. Water temperature in the thermal reservoir for configuration I: (Polycarbonate)

This graph shows the water temperature stored in the thermal reservoir over time. The data indicates the effectiveness of the Polycarbonate-covered solar collector in maintaining water temperature, with fluctuations reflecting the balance between heat input from the collector and heat losses from the reservoir. The lower temperatures compared to the Glass configuration suggest that the Polycarbonate cover is less effective in maintaining high water temperatures due to higher thermal losses.

The temperature of the upper outer surface of the absorber plate was measured by five thermocouples distributed at five different points to evaluate the temperature distribution in the plate. The graph in Figure 10 shows hourly mean values for each point of the absorber plate for configuration I (Oliveira & Charamba Dutra, 2023). Temperatures average 3-5°C lower than the Glass cover, aligning with lower efficiency. Uniform heating is demonstrated across

positions T1-T5, but T3 at the center lags due to edge heat losses. The lower average temperatures suggest the Polycarbonate cover allows more heat to escape, reducing the system's overall efficiency.

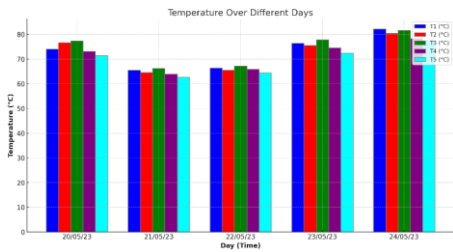


Figure 10. Average hourly temperatures at the five points of the absorber plate for configuration I (Polycarbonate)

This graph presents the temperature distribution across the absorber plate, highlighting the uniformity of heat absorption and transfer. The lower temperatures compared to the Glass cover suggest higher thermal losses and lower efficiency in the Polycarbonate configuration. The consistent lower temperatures across the plate indicate that the Polycarbonate cover does not retain heat as effectively as glass.

The outlet temperature of the collector has always been above 40.4°C, with the highest hourly average recorded being 43°C. The inlet temperature of the collector at the beginning of the test was always close to the external ambient temperature but reached a daily average of 34.7°C. The maximum temperature gradient obtained in the water by the circulation in the collector was 9.1°C, with a mean value of 8.7°C, as shown in Figure 11.

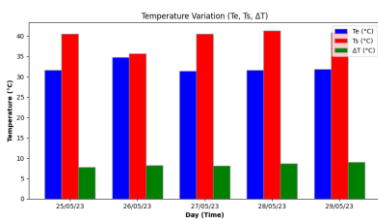


Figure 11. Average hourly temperatures of the collector's inlet and outlet and the temperature variation of the water in the collector for configuration II: (GLASS)

This Figure illustrates the temperature variation of the water in the solar collector with a Glass cover, showing the heat transfer efficiency from the absorber plate to the circulating fluid. The higher temperature gradients compared to the Polycarbonate

configuration indicate better performance. The superior thermal properties of glass, such as higher optical transmittance and lower thermal emittance, result in more effective heat absorption and transfer to the fluid.

The average efficiency of the collector in this configuration for the tested days was always above 45.6%, reaching a daily average of 56%. Still, the average hourly value for the five days was around 50.5%. The graph in Figure 12 shows the behavior assumed by the hourly averages of the thermal efficiency for configuration II.

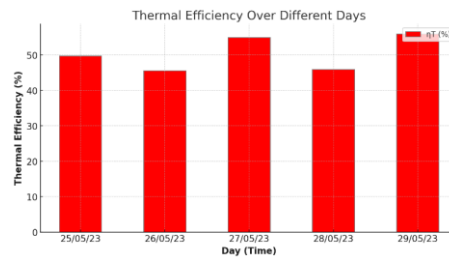


Figure 12. Hourly averages of thermal efficiency for configuration II: (Glass)

This graph presents the thermal efficiency of the solar collector with the Glass cover, highlighting the system's ability to convert solar energy into usable heat. The higher average efficiency compared to the Polycarbonate configuration underscores the superior performance of the Glass cover. The glass cover's higher efficiency is due to its better optical and thermal properties, allowing for greater heat retention and transfer.

The average global solar radiation for the test days in this configuration was around 884.2 W/m². The graph in Figure 13 shows the behavior assumed by the hourly averages of global solar radiation for configuration II.

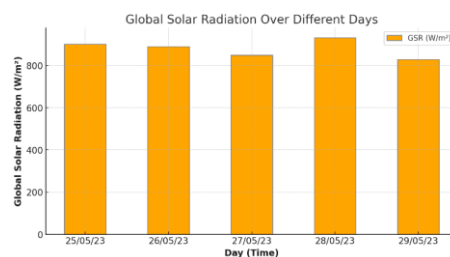


Figure 13. Hourly averages of global solar radiation for configuration II: (Glass)

This graph displays the solar radiation received by the solar collector with a Glass cover, providing a basis for comparing the performance of the two

configurations under similar solar energy conditions. The slightly higher average irradiation compared to the Polycarbonate configuration ensures that the performance comparisons are fair and consistent.

The thermal reservoir that stores the water heated by the collector for the tested days provided hot water with an average temperature of 37.2°C, above the temperature considered ideal for bathing, around 34°C. The graph in Figure 14 shows the behavior assumed by the water temperature in the thermal reservoir [37].

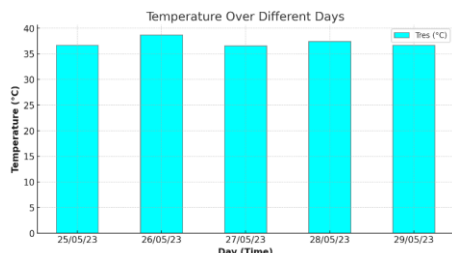


Figure 14. Water Temperature in the Thermal Reservoir for Configuration II (Glass)

This graph shows the water temperature in the thermal reservoir for the glass-covered configuration, indicating the system's ability to maintain higher water temperatures than the polycarbonate configuration. This reflects the Glass cover's better thermal performance and heat retention properties. The higher water temperatures are due to the glass cover's ability to minimize thermal losses and retain more heat within the system.

The temperature of the upper outer surface of the absorber plate was measured through five thermocouples distributed at five different points to evaluate the temperature distribution in the plate. The graph in Figure 15 shows hourly mean values for each point of the absorber plate for configuration II.

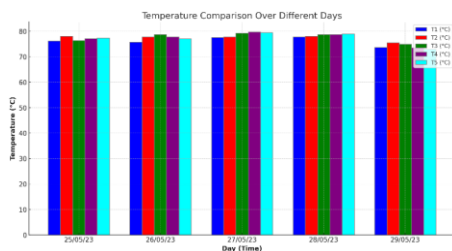


Figure 15 Temperature in the 05 points distributed on the absorber plate for configuration II: (Glass)

This graph presents the temperature distribution across the absorber plate for the Glass-covered configuration. The uniform temperature profile indicates efficient heat absorption and transfer,

contributing to the system's overall higher thermal efficiency. The consistently higher temperatures across the plate suggest that the Glass cover is more effective in retaining and distributing heat.

The equipment available to carry out this research did not allow the ideal assembly of the experiment, that is, the placement of a system working with the Polycarbonate cover side by side with another system working with the Glass cover, with the same physical characteristics (mounting, solar collectors, thermal reservoir, and pipes) subjected to the same climatic conditions. A single system was installed, and tests were carried out on alternate days to obtain homogeneous conditions of the test and climatic variables between the two system covers. Initially, when comparing the tests, it can be said that the heating system achieved homogeneous results under very similar climatic conditions in several thermal parameters in the two configurations studied. The graphs in Figures 16 and 17 show the average efficiency and radiation for the two configurations studied.

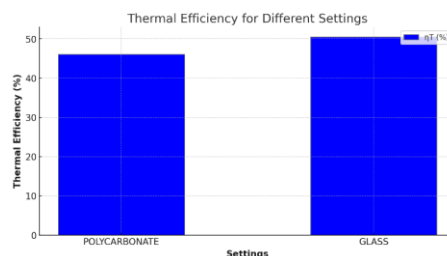


Figure 16. Average thermal efficiency for the two configurations (Polycarbonate and Glass)

This graph compares the average thermal efficiency of the solar collector for both Polycarbonate and Glass configurations, highlighting the differences in performance and identifying which cover material is more effective in converting solar energy into heat. The glass cover's higher efficiency is attributed to its superior optical and thermal properties, which result in better heat retention and transfer.

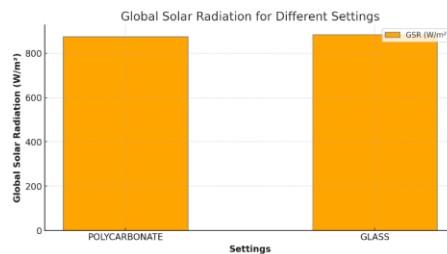


Figure 17. Average solar radiation for the two configurations (Polycarbonate and Glass)

This graph shows the average solar radiation received during the tests for both configurations. It provides a basis for comparing the performance of the solar collectors under similar solar energy conditions and highlights the consistency of solar irradiance during the test days. The slightly higher average irradiation for the Glass configuration ensures that the performance comparisons are fair and consistent.

Configuration I (Polycarbonate), which received slightly lower radiation than in configuration II (Glass) (874.6 W/m^2 versus 884.2 W/m^2), it also achieved a lower performance. This significantly different result occurred because of the test day (20/05/23), a day of lower solar radiation (750 W/m^2) in which clouds shaded the collector. By reducing the incidence of direct radiation, this period was more prolonged, thus causing a drop in the temperatures of the plate, entrance, and exit of the fluid in the collector, decreasing heat transfer [38]. Comparing the two configurations in which the days were subjected to solar radiation values more approximately, it is possible to compare the days (12/23/2014 glass) and (21/05/23 Polycarbonate). Similar results were presented in almost all thermal parameters; the system's efficiency for this day in favor of glass was only 0.9% [39]. On the day (22/05/23 Polycarbonate), it became interesting to compare the results achieved because, on this day, there were no clouds to interfere with the performances in almost all thermal parameters. This was the day that reached the highest solar radiation index (981 W/m^2). The plates were changed, and on the day (28/05/23 glass), the global solar radiation values for this day reached 952 W/m^2 . Comparing the day (23/05/23 Polycarbonate) with the day (29/05/23 glass), a 29 W/m^2 higher amount of radiation, the difference in efficiency for the two configurations was 2.2% in favor of glass. Comparing the day (25/05/23 Polycarbonate, radiation of 834 W/m^2) against the day (28/05/23 glass, radiation of 829 W/m^2), we obtained a 12.4% higher efficiency index in favor of glass.



Figure 18. Polycarbonate cover

Figure 18 shows the result of the Polycarbonate roofing after around 10 months of sun exposure in the

proposed solar system. According to the manufacturer's specifications, the Polycarbonate sheet has a 10-year warranty against yellowing and loss of light transmission. Still, the related change in the material's opacity was noticeable, showing a change in color at the end of the test. Regarding the efficiency of this plate, no changes were observed in the short term since the temperature values incident on it were similar before and after [40]. The degradation in the Polycarbonate cover indicates potential long-term issues with durability and optical performance, which could impact its effectiveness as a solar collector glazing material.

In both cases, configuration I and configuration II confirm a better performance (albeit small) for the enclosed solar system using glass for roofing. Regarding the stratification of the water in the thermal reservoir, although the temperature control was made at only one point inside the thermal reservoir (thermocouple inserted at the top), it was possible to evaluate the temperature levels for all the tests of the two configurations studied, demonstrating the feasibility of the proposed solar collector to provide hot water for bathing with a temperature above 37°C for both configurations [41]. The better performance of the Glass cover can be attributed to its superior optical and thermal properties, which result in better heat retention and transfer, leading to higher overall efficiency.

The superior thermal performance of the glass-covered solar collector can be attributed to several interrelated factors revealed through in-depth analysis of the experimental data [42]. The higher transmittance of solar irradiation for glass allows the collector absorber plate to absorb more energy. Glass has a smooth surface and undergoes less light scattering than the more textured Polycarbonate. The glass cover showed $\sim 90\%$ transmittance over the solar spectrum based on optical characterization versus $\sim 85\%$ for Polycarbonate. This optical advantage translates directly to higher thermal energy gain.

The observed absorber plate temperatures were $3\text{--}5^\circ\text{C}$ higher on average for the glass configuration. The glass cover radiates less thermal energy outwards, maintaining more heat at the absorber. The smooth glass surface has a lower infrared emissivity of 0.9 compared to 0.95 for Polycarbonate. The lower emittance reduces radiative heat losses to the ambient air, keeping absorbed energy within the system [43].

The air gap between the cover and absorber in both collectors restricts convective losses. However, the glass cover maintained a consistently higher temperature gradient between the absorber and the

cover. This indicates the smoother glass surface disrupted the air gap conduction and convection slightly less than the rougher Polycarbonate, further minimizing heat losses.

Higher absorber plate temperatures in the glass-covered collector facilitated greater conductive heat transfer to the fluid pipes. The average 8.7°C fluid heating for glass versus 8.1°C for Polycarbonate demonstrates this. The sustained thermal energy within the all-glass system enabled more efficient harvesting [44].

No visible degradation or discoloration occurred in the glass cover during testing. In contrast, the Polycarbonate showed some faint scratching and yellowing after just ten months. This suggests long-term optical instability in Polycarbonate that could substantially lower performance over years of operation.

The glass cover configuration maintained solar energy absorption and retention within the collector more effectively through superior optical transmittance, lower radiative losses, less convective disruption, better absorber heat transfer, and durable transparency. The inherent material properties and behavior can explain the quantitative performance differences.

6. Conclusion

This experimental investigation aimed to compare the thermal efficiency of flat plate solar collectors using Polycarbonate and Glass covers for solar water heating applications in India. The key findings from this study are as follows:

The glass-covered configuration exhibited a 4.4% higher average thermal efficiency, reaching 50.5%, compared to the polycarbonate-covered configuration, which achieved 46.1%. The higher efficiency of the glass cover is attributed to its superior optical and thermal properties, allowing better heat retention and transfer.

The maximum water temperature increase was slightly greater with the glass cover (9.1°C) than the Polycarbonate cover (8.7°C). This suggests the glass cover facilitates more efficient heat transfer to the working fluid.

Despite the slight variations in solar irradiance on different test days, the glass cover consistently outperformed the Polycarbonate cover. The stability

of the glass material under prolonged exposure to sunlight contributed to its superior performance.

The Polycarbonate cover showed signs of yellowing and scratching after 10 months of exposure, indicating potential long-term durability issues. In contrast, the glass cover maintained its transparency and structural integrity, ensuring consistent performance.

While Polycarbonate offers a lower initial cost, the superior thermal efficiency and durability of glass covers may justify the higher investment, leading to better long-term performance and reliability.

Future research should focus on long-term performance and durability assessments of Polycarbonate covers under various climatic conditions to establish their viability as an economical alternative to glass. Additionally, exploring advanced coatings for Polycarbonate that enhance its optical and thermal properties could further improve its efficiency. Investigating the impact of different tilt angles and orientations on collector performance will help optimize system design for maximum efficiency. Comparative studies involving other potential cover materials, such as acrylic or glass-polymer composites, may reveal additional cost-effective solutions. Finally, a comprehensive economic analysis, including the payback period of solar water heating systems with various cover materials, will provide valuable insights for broader adoption in residential and commercial applications. These future directions will contribute to optimizing flat plate solar collector designs and expanding sustainable water heating solutions across diverse environments.

Nomenclature

Parameter	Description
T_o	Outlet temperature of the collector (°C)
T_i	Inlet temperature of the collector (°C)
ΔT	Temperature gain (°C)
A_c	Collector surface area (m ²)
G	Solar irradiance (W/m ²)
Q_u	Useful energy gain (W)
η	Thermal efficiency (%)
m	Mass flow rate (kg/s)
c_p	Specific heat capacity of the fluid (J/kg·K)
I	Solar irradiance intensity (W/m ²)
T_{amb}	Ambient temperature (°C)
T_{plate}	Absorber plate temperature (°C)

U	Overall heat loss coefficient (W/m ² ·K)
FR	Collector heat removal factor
F'	Collector efficiency factor
η_0	Optical efficiency of the collector (%)
τ	Transmittance of the glazing material
α	Absorptance of the absorber plate
ε	Emittance of the glazing material
Δ_I	Error in solar irradiation
Δ_A	Error in collector surface area
Δ_{Qu}	Error in useful energy gain
Δ_η	Error in overall thermal efficiency
Δ_{in}	Error in mass flow rate
Δ_{cp}	Error in specific heat capacity
$\Delta_{T_{out}}$	Error in outlet temperature
$\Delta_{T_{in}}$	Error in inlet temperature

References

- [1] Abdelsalam, E., Almomani, F., Azzam, A., Juaidi, A., Abdallah, R., & Shboul, B. (2024). Synergistic energy solutions: Solar chimney and nuclear power plant integration for sustainable green hydrogen, electricity, and water production. *Process Safety and Environmental Protection*, 186, 756–772. <https://doi.org/10.1016/j.psep.2024.03.121>
- [2] Abedi, M., Tan, X., Saha, P., Klausner, J. F., & Bénard, A. (2024). Design of a solar air heater for a direct-contact packed-bed humidification–dehumidification desalination system. *Applied Thermal Engineering*, 244, 122700. <https://doi.org/10.1016/j.applthermaleng.2024.122700>
- [3] Attia, M. E. H., Kabeel, A. E., Khelifa, A., & Abdel-Aziz, M. M. (2024). Thermal and electrical analysis of the performance of a skeleton-shaped tubes via hybrid PVT cooling system. *Applied Thermal Engineering*, 248, 123277. <https://doi.org/10.1016/j.applthermaleng.2024.123277>
- [4] Beltrán, F., Sommerfeldt, N., Eskola, J., & Madani, H. (2024). Empirical investigation of solar photovoltaic-thermal collectors for heat pump integration. *Applied Thermal Engineering*, 248, 123175. <https://doi.org/10.1016/j.applthermaleng.2024.123175>
- [5] Diao, Y., Gong, X., Xu, D., Duan, P., Wang, S., & Guo, Y. (2024). From culture, harvest to pretreatment of microalgae and its high-value utilization. *Algal Research*, 78, 103405. <https://doi.org/10.1016/j.algal.2024.103405>
- [6] Duraivel, B., Muthuswamy, N., & Gnanavendan, S. (2024). Comprehensive analysis of the greenhouse solar tunnel dryer (GSTD) using Tomato, snake Gourd, and Cucumber: Insights into energy Efficiency, exergy Performance, economic Viability, and environmental impact. *Solar Energy*, 267, 112263. <https://doi.org/10.1016/j.solener.2023.112263>
- [7] Hashemi, S. F., Pourfallah, M., & Gholinia, M. (2024). Thermal performance enhancement in an indirect solar greenhouse dryer using helical fin under variable solar irradiation. *Solar Energy*, 267, 112217. <https://doi.org/10.1016/j.solener.2023.112217>
- [8] Johnson, Z. S., Abakar, Y. A., Caleb, N. N., & Chen, B. (2024). An open-loop hybrid photovoltaic solar thermal evacuated tube energy system: A new configuration to enhance techno economic of conventional photovoltaic solar thermal system. *Journal of Building Engineering*, 82, 108000. <https://doi.org/10.1016/j.job.2023.108000>
- [9] Kotkondawar, A., Gabhane, K., & Rayalu, S. (2024). Design and performance evaluation of Front glass-covered photovoltaics-thermal hybrid system for enhanced electrical output and hot water production. *Measurement: Energy*, 100006. <https://doi.org/10.1016/j.meae.2024.100006>
- [10] Noman, S., & Manokar, A. M. (2024). Experimental investigation of pistachio shell powder (bio-waste) to augment the performance of tubular solar still: Energy, exergy, and environmental analysis. *Desalination*, 576, 117317. <https://doi.org/10.1016/j.desal.2024.117317>
- [11] Partheeban, P., Jegadeesan, V., Manimuthu, S., & Chella Gifta, C. (2024). Cleaner production of geopolymer bricks using Solar-LPG hybrid dryer. *Journal of Cleaner Production*, 442, 141048. <https://doi.org/10.1016/j.jclepro.2024.141048>
- [12] Ammar, M., Mokni, A., Mhiri, H., & Bournot, P. (2020). Numerical analysis of solar air collector provided with rows of rectangular fins. *Energy Reports*, 6, 3412–3424. <https://doi.org/10.1016/j.egy.2020.11.252>
- [13] Shabahang Nia, E., & Ghazikhani, M. (2024). Enhancing reliability and efficiency of solar chimney by phase change material Integration: An Experimental study. *Thermal Science and Engineering Progress*, 51, 102600. <https://doi.org/10.1016/j.tsep.2024.102600>
- [14] Struchalin, P. G., Zhao, Y., & Balakin, B. V. (2024). Field study of a direct absorption solar collector with eco-friendly nanofluid. *Applied Thermal Engineering*, 243, 122652. <https://doi.org/10.1016/j.applthermaleng.2024.122652>
- [15] Thangaraj, H., Winston David, P., Raj, M., & Babu Balachandran, G. (2024). Performance of stand-alone bifacial photovoltaic module using non-biodegradable waste as reflectors for

- tropical climatic region of southern India: An experimental approach. *Solar Energy*, 268, 112302.
<https://doi.org/10.1016/j.solener.2023.112302>
- [16] Wang, J., Luo, Q., Cheng, J., Qu, M., Wang, P., Zhao, S., Xu, H., & Ma, C. (2024). Study on thermal property of a solar collector applied to solar greenhouse. *Applied Thermal Engineering*, 244, 122628.
<https://doi.org/10.1016/j.applthermaleng.2024.122628>
- [17] Zheng, J., Febrer, R., Castro, J., Kizildag, D., & Rigola, J. (2024). A new high-performance flat plate solar collector. Numerical modelling and experimental validation. *Applied Energy*, 355, 122221.
<https://doi.org/10.1016/j.apenergy.2023.122221>
- [18] Das, B., Mondol, J. D., Negi, S., Smyth, M., & Pugsley, A. (2021). Experimental performance analysis of a novel sand coated and sand filled polycarbonate sheet based solar air collector. *Renewable Energy*, 164, 990–1004.
<https://doi.org/10.1016/j.renene.2020.10.054>
- [19] Yadav, M. K., Kedare, S. B., & Modi, A. (2023). Experimental investigation of a compound parabolic concentrator with aerogel and polycarbonate cover. *Applied Thermal Engineering*, 121585.
<https://doi.org/10.1016/j.applthermaleng.2023.121585>
- [20] Ammar, M., Mokni, A., Mhiri, H., & Bournot, P. (2021). Performance optimization of flat plate solar collector through the integration of different slats arrangements made of transparent insulation material. *Sustainable Energy Technologies and Assessments*, 46.
<https://doi.org/10.1016/j.seta.2021.101237>
- [21] Belkhode, P. N., Shelare, S. D., Sakhale, C. N., Kumar, R., Shanmugan, S., Soudagar, M. E. M., & Mujtaba, M. A. (2021). Performance analysis of roof collector used in the solar updraft tower. *Sustainable Energy Technologies and Assessments*, 48.
<https://doi.org/10.1016/j.seta.2021.101619>
- [22] Chandan, Suresh, V., Iqbal, S. M., Reddy, K. S., & Pesala, B. (2021). 3-D numerical modelling and experimental investigation of coupled photovoltaic thermal and flat plate collector. *Solar Energy*, 224, 195–209.
<https://doi.org/10.1016/j.solener.2021.05.079>
- [23] Channa Keshava Naik, N., Shashi Shekar, K. S., Gautham, M. G., & Prasad, T. B. (2021). Comparative study of pebble absorber solar thermal collector (PASTC) with conventional absorber solar thermal collector (CASTC). *Materials Today: Proceedings*, 46, 2641–2646.
<https://doi.org/10.1016/j.matpr.2021.02.354>
- [24] Hassan, H., Osman, O. O., Abdelmoez, M. N., & abo-Elfadl, S. (2023). Experimental assessment of novel designed solar hot water storage collector incorporating an array of partitioned ducts absorber. *Solar Energy*, 262.
<https://doi.org/10.1016/j.solener.2023.111838>
- [25] Jiang, Y., Zhang, H., You, S., Fan, M., Wang, Y., & Wu, Z. (2021). Dynamic performance modeling and operation strategies for a v-corrugated flat-plate solar collector with movable cover plate. *Applied Thermal Engineering*, 197.
<https://doi.org/10.1016/j.applthermaleng.2021.117374>
- [26] Kandasamy, V. K., Jaganathan, S., Dhairiyasamy, R., & Rajendran, S. (2023). Optimizing the efficiency of solar thermal collectors and studying the effect of particle concentration and stability using nanofluidic analysis. *Energy*, 34(5), 1564–1591.
<https://doi.org/10.1177/0958305X231183687>
- [27] Kizildag, D., Castro, J., Kessentini, H., Schillaci, E., & Rigola, J. (2022). First test field performance of highly efficient flat plate solar collectors with transparent insulation and low-cost overheating protection. *Solar Energy*, 236, 239–248.
<https://doi.org/10.1016/j.solener.2022.02.007>
- [28] Lamrani, B., Elmrbet, Y., Mathew, I., Bekkioui, N., Etim, P., Chahboun, A., Draoui, A., & Ndukwu, M. C. (2022). Energy, economic analysis and mathematical modelling of mixed-mode solar drying of potato slices with thermal storage loaded V-groove collector: Application to Maghreb region. *Renewable Energy*, 200, 48–58.
<https://doi.org/10.1016/j.renene.2022.09.119>
- [29] Miao, R., Hu, X., Yu, Y., Zhang, Y., Wood, M., & Olson, G. (2021). Experimental study of a newly developed dual-purpose solar thermal collector for heat and cold collection. *Energy and Buildings*, 252.
<https://doi.org/10.1016/j.enbuild.2021.111370>
- [30] Miao, R., Hu, X., Yu, Y., Zhang, Y., Wood, M., Olson, G., & Yang, H. (2022). Evaluation of cooling performance of a novel dual-purpose solar thermal collector through numerical simulations. *Applied Thermal Engineering*, 204.
<https://doi.org/10.1016/j.applthermaleng.2021.117966>

- [31] Nishit, J., & Bekal, S. (2023). Experimental investigation on polymer solar water heater using Al₂O₃ nanofluid for performance improvement. *Materials Today: Proceedings*. <https://doi.org/10.1016/j.matpr.2023.04.475>
- [32] Oliveira, M., & Charamba Dutra, J. C. (2023). The impact of the V-corrugation on the thermal efficiency of a solar collector. *Solar Energy*, 255, 460–473. <https://doi.org/10.1016/j.solener.2023.02.053>
- [33] Radwan, A., Abdelrehim, O., Salem, M. S., Abo-Zahhad, E. M., Elmarghany, M. R., Shouman, M. A., & Khater, A. (2023). A modified support pillar design for a flat vacuum-based solar thermal collectors. *Sustainable Energy Technologies and Assessments*, 58. <https://doi.org/10.1016/j.seta.2023.103372>
- [34] Radwan, A., Abo-Zahhad, E. M., El-Sharkawy, I. I., Said, Z., Abdelrehim, O., Memon, S., Cheng, P., & Soliman, A. S. (2024). Thermal analysis of a bifacial vacuum-based solar thermal collector. *Energy*, 294, 130748. <https://doi.org/10.1016/j.energy.2024.130748>
- [35] Ramdani, H., & Ould-Lahoucine, C. (2020). Study on the overall energy and exergy performances of a novel water-based hybrid photovoltaic-thermal solar collector. *Energy Conversion and Management*, 222. <https://doi.org/10.1016/j.enconman.2020.113238>
- [36] Sharma, K., Kumar, V., Bisht, D. S., & Garg, H. (2021). Comparative study of acrylic flat plate and dome shaped collector for summer and winter solstice conditions. *Materials Today: Proceedings*, 45, 5489–5493. <https://doi.org/10.1016/j.matpr.2021.02.200>
- [37] Herrando, M., Fantoni, G., Cubero, A., Simón-Allué, R., Guedea, I., & Fueyo, N. (2023). Numerical analysis of the fluid flow and heat transfer of a hybrid PV-thermal collector and performance assessment. *Renewable Energy*, 209, 122–132. <https://doi.org/10.1016/j.renene.2023.03.125>
- [38] Tarmenzi, M. A. S. M., Razak, A. A., Azmi, M. A. A., Fazlizan, A., Majid, Z. A. A., & Sopian, K. (2021). Comparative study on thermal performance of cross-matrix absorber solar collector with series and parallel configurations. *Case Studies in Thermal Engineering*, 25. <https://doi.org/10.1016/j.csite.2021.100935>
- [39] Tripanagnostopoulos, Y., Huang, G., Wang, K., & Markides, C. N. (2022). 3.08 - Photovoltaic/Thermal Solar Collectors. *Comprehensive Renewable Energy*, Second Edition: Volume 1-9, 1–3, 294–345. <https://doi.org/10.1016/B978-0-12-819727-1.00051-0>
- [40] Vahidinia, F., & Khorasanizadeh, H. (2021). Development of new algebraic derivations to analyze minichannel solar flat plate collectors with small and large size minichannels and performance evaluation study. *Energy*, 228. <https://doi.org/10.1016/j.energy.2021.120640>
- [41] Wang, T., Diao, Y., Zhao, Y., Liang, L., Wang, Z., & Chen, C. (2020). A comparative experimental investigation on thermal performance for two types of vacuum tube solar air collectors based on flat micro-heat pipe arrays (FMHPA). *Solar Energy*, 201, 508–522. <https://doi.org/10.1016/j.solener.2020.03.024>
- [42] Yan, S. R., Golzar, A., Sharifpur, M., Meyer, J. P., Liu, D. H., & Afrand, M. (2020). Effect of U-shaped absorber tube on thermal-hydraulic performance and efficiency of two-fluid parabolic solar collector containing two-phase hybrid non-Newtonian nanofluids. *International Journal of Mechanical Sciences*, 185. <https://doi.org/10.1016/j.ijmecsci.2020.105832>
- [43] Hashemian, N., & Noorpoor, A. (2019). Assessment and multi-criteria optimization of a solar and biomass-based multi-generation system: Thermodynamic, exergoeconomic and exergoenvironmental aspects. *Energy Conversion and Management*, 195, 788–797. <https://doi.org/10.1016/j.enconman.2019.05.039>
- [44] Hashemian, N., & Noorpoor, A. (2023). Thermo-eco-environmental investigation of a Newly Developed Solar/wind Powered Multi-Generation Plant with Hydrogen and Ammonia Production Options. *Journal of Solar Energy Research*, 8(4), 1728–1737. doi: 10.22059/jser.2024.374028.1388